

First principles studies of the graphene-phenol interactions

José M. Galicia Hernández · Ernesto Chigo Anota ·
María T. Romero de la Cruz ·
Minerva González Melchor ·
Gregorio Hernández Cocoltzi

Received: 26 November 2011 / Accepted: 14 February 2012 / Published online: 14 March 2012
© Springer-Verlag 2012

Abstract Studies of the interaction between phenol and intrinsic graphene, as well as phenol and aluminum doped graphene layer are performed using first principles total energy calculations within the periodic density functional theory. A 4x4 periodic structure is used to explore the adsorption of a phenol molecule on the intrinsic graphene and on aluminum doped graphene layer. The electron-ion interactions are modeled using ultra-soft pseudo-potentials, and the exchange-correlation energies are treated according to the generalized gradient approximation (GGA) with the PBE parameterization. We consider different molecule orientations: parallel and perpendicular to the graphene layer to relax the atomic structure. To explain the optimized atomic geometry we determine binding energies for all cases and the density of

states (DOS) and partial DOS for the most relevant configurations. Results indicate that the direct interaction of oxygen with aluminum yields the ground state geometry with the phenol molecule adsorbed on the graphene layer. Binding energies and DOS structures also demonstrate that the ground state configuration is that where the O and Al atoms interact with a separation distance of 1.97 Å.

Keywords Density functional theory ·
First principles calculations · Graphene · Phenol

Introduction

Graphene is an allotrope of carbon in which, the atoms arranged in a 2D honeycomb structure form a slightly rippled layer of one atom thickness, it has been the subject of many experimental as well as theoretical investigations, since its discovery in 2004 [1]. This recently discovered and prepared material has a large number of possible technological applications. Graphene is considered the reference for all sp^2 -derived allotropic forms of carbon (graphite, fullerenes, nanotubes, schwarzite). Far reaching applications such as patterned single-electron transistors [2] and ultimate gas sensors able to detect one molecule [3] have been envisioned. Geim et al. have fabricated graphene flakes by micromechanical cleavage of graphite [1]. Graphene deposits have also been produced by SiC epitaxy [4]. Both techniques are limited in terms of quantities of available samples.

Phenol (C_6H_5OH), also known as phenyl acid or carboic acid [5], has a non-alcohol atomic structure with functional group Ph-OH, which is different from that of alcohol, R-OH. It is mainly used to produce resins, nylon, synthetic fibers, agrochemicals, polycarbonates and acetylsalicylic acid (aspirin). C_6H_5OH is employed in the preparation of

J. M. G. Hernández (✉) · M. G. Melchor · G. H. Cocoltzi
Instituto de Física ‘Luis Rivera Terrazas’,
Benemérita Universidad Autónoma de Puebla,
Apartado Postal J-48,
Puebla 72570, Mexico
e-mail: josemariogahe@hotmail.com

M. G. Melchor
e-mail: minerva@ifuap.buap.mx

G. H. Cocoltzi
e-mail: cocoltzi@ifuap.buap.mx

E. C. Anota
Benemérita Universidad Autónoma de Puebla,
Facultad de Ingeniería Química,
Ciudad Universitaria, San Manuel,
Puebla 72570, Mexico
e-mail: echigoa@yahoo.es

M. T. R. de la Cruz
Universidad Autónoma de Coahuila,
Facultad de Ciencias Físico-Matemáticas,
Saltillo, Coahuila 25280, Mexico
e-mail: tere@ifuap.buap.mx

orally cleaning liquids and pills to cure sore throat. It is also used as fungicide, antibacterial [6], antiseptic and disinfectant in the chemistry, pharmacy and clinic industries [7–9]. However, phenol is a contaminant in products like wastewater [10–12]. The search for efficient adsorbents of small gas molecules is driven by needs for ultraclean air environment and by a danger related to easy availability of toxic industrial gases. Therefore in this work we address the problem of studying the phenol adsorption on the hexagonal graphene, in order to search for a material suitable to remove contaminants. The problem in the removal of contaminant gases lies in the small size of their molecules and weak interactions with the surface of adsorbents via physical forces [13]. Moreover, in real life applications, adsorption is expected to clean environment. Experiments have shown that graphite derived materials can adsorb hydrogen sulfide [13, 14].

Recent studies have suggested graphene as a good adsorbent material of organic molecules. For instance, first principles total energy calculations performed by Leenaerts et al. [3] have demonstrated that H₂O, NH₃, CO, NO₂ and NO can be adsorbed on graphene with adsorption energies of the order of meV. Chi et al. [15] have shown that formaldehyde (an organic molecule) can be adsorbed on intrinsic and Al-doped graphene. Binding energies in the former case are of the order of meV, while in the latter case the energies are of the order of eV. It is evident that the adsorption energy is favored by the doping of the graphene layer. These studies also show that graphene can be used as a gas sensor provided it has the ability to detect even single molecules. Additionally graphene is a material sensitive to changes in the charge distribution which lead to a variation in the electrical resistivity.

On the other hand, recent studies by Chakarova-Käck et al. [16] indicate that phenol can be adsorbed on graphite. The model of graphite used in the studies consists of a single carbon monolayer (graphene) with results indicating that there are no significant changes in the adsorption energies if the interaction of phenol with other layers is considered. In all previous studies, adsorption energies are of the order of meV in agreement with our calculations, therefore it can be concluded that graphene may adsorb phenol.

Provided that the adsorption of molecules on graphene show energies of the order of meV, it is desirable to increase these energies. It has been demonstrated that one way to increase the adsorption energies is by doping graphene with aluminum. Considering Al-doped graphene, studies of the adsorption of formaldehyde and CO on graphene have been performed with results showing an increase in the binding energies [15, 17]. Similarly it is intended to use Al-doped graphene to create an efficient and controllable adsorption/desorption system for hydrogen storage.

To investigate the interaction between graphene and phenol, and the aluminum doped graphene and phenol we have

performed first principles total energy calculations applying the periodic density functional theory. The understanding of these interactions will help to suggest possible ways to remove or separate and turn these molecules into products with low environmental impact, achieving a minimum of emission into the atmosphere. The paper is organized as follows: In Sect. 2 we describe the method of calculations. Section 3 is devoted to describing and discussing results, and in Sect. 4 we make conclusions.

Calculation models and methods

First principles total energy calculations are performed to study the graphene-phenol and the aluminum doped graphene-phenol interactions. Calculations are done within the periodic density functional theory as implemented in the PWscf code of the Quantum ESPRESSO package [18]. The exchange-correlation energies are treated according to the generalized gradient approximation (GGA) with the PBE [19] parameterization and the electron-ion interactions are treated with ultra-soft pseudopotentials. To model the surface we have employed the supercell method, which is composed of a graphene layer and a vacuum gap of 20 Å to prevent interactions between adjacent layers. The one atom thick, 2-D array of carbon hexagons graphene is considered in a 4x4 periodic array, upon which phenol is supposed to be adsorbed. Two cases are mainly explored: In the *first case* we deal with the interaction between intrinsic graphene and phenol and in the *second case* we consider the aluminum doped graphene layer in order to investigate its interaction with phenol. Several atomic configurations are studied: In the first set of atomic geometries the phenol molecule is parallel to the graphene layer and in the second set the molecule is perpendicular to the graphene layer. Calculations start with the graphene lattice parameter optimization (we have obtained a value of 2.47 Å), then this is followed by the atomic structure relaxation of the phenol adsorption and at the final stage we calculate the charge density distribution and the density of states, taking into account the relaxed atomic coordinates. The electron states and electron density are expanded in plane waves with an energy cut of 30 Ry and 240 Ry, respectively. A 6x6x1 k-points mesh is used in our calculations. This set has been proven to be enough to obtain trustable results since increasing the mesh yields small differences in the binding energies, but an increase in the computing time [20].

Results and discussion

Studies of the graphene—phenol, and aluminum doped graphene—phenol interactions are presented in this section.

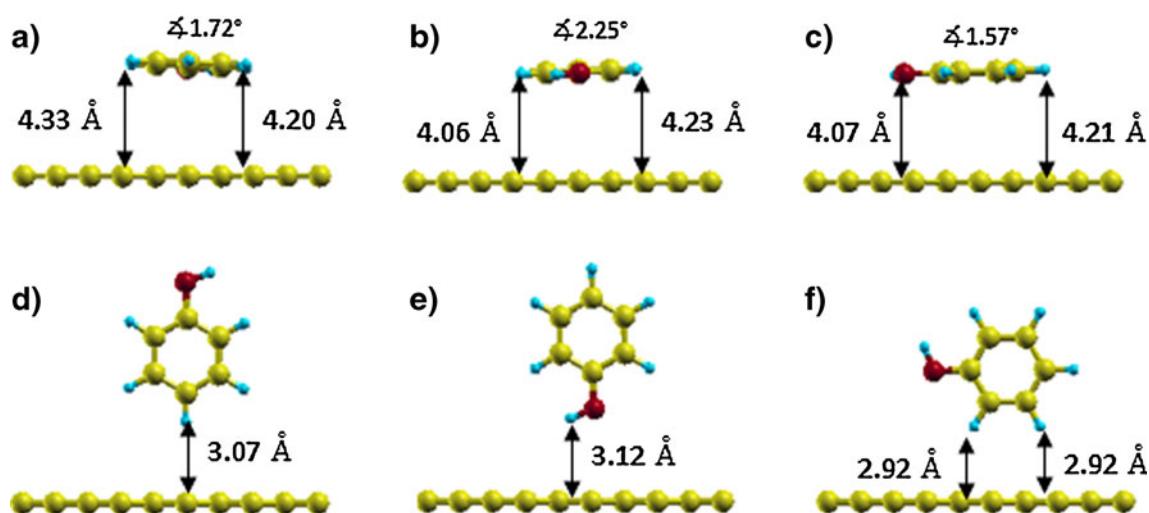


Fig. 1 In this figure we show the relaxed structures for all configurations of phenol molecule interacting with the intrinsic graphene; (a) A1, (b) A2, (c) A3, (d) A4, (e) A5 and (f) A6

To present results we first consider the interaction of intrinsic graphene with phenol in two set of configurations: the molecule parallel to the graphene layer and the molecule perpendicular to the layer, on the other hand, we consider the aluminum doped graphene interacting with phenol in the same sets of configurations described above.

Geometry optimization

Our calculations started with the geometry optimization for all cases. Figure 1 shows the optimized geometries for the graphene - phenol configurations, in the parallel geometries we have obtained that the average separation distance between phenol and graphene is larger than 4 Å, consequently we conclude that no chemical bonds take place, instead physical interactions are present. Similarly, in the perpendicular configurations we have obtained that the separation distance between phenol and graphene is of the order of 3 Å, which indicates that the possible adsorption is of the physisorption type.

Despite the smaller separation distances between phenol and graphene in perpendicular configurations, calculations of the binding energies show that these are larger in the

parallel geometries, which are of the order of 80 meV (see Table 1). Clearly the energy values demonstrate that we only obtain physisorption. These results are in contrast to the interaction of phenol with the aluminum doped graphene layer, as described below.

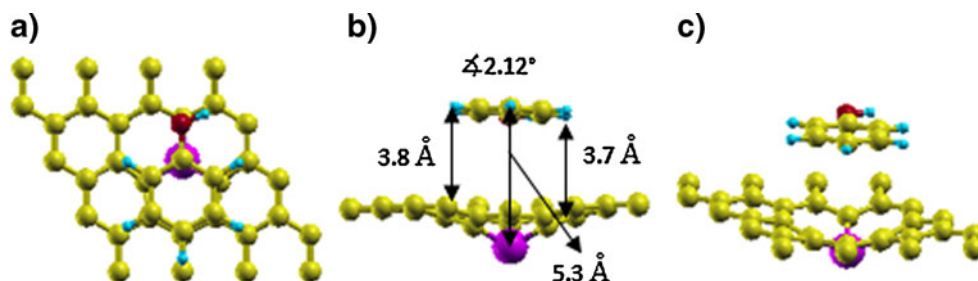
Studies of the interaction of phenol with the aluminum doped graphene are presented in different atomic configurations. We shall consider the interactions of graphene with phenol in two sets of configurations; in the first set the molecule will be parallel and in the second perpendicular to graphene. We describe first the parallel configurations. In Fig. 2 we present the relaxed model B1 of a parallel geometry, in a) we display the top view, in b) and c) the side views. The top view of the geometry B1 shows the hexagon of the phenol molecule on top of a hexagon of the graphene layer. One carbon is on top of the aluminum and the oxygen is on top of one carbon of the layer. After the relaxation the resulting configuration is somewhat distorted from the original parallel geometry, the planar configuration of the doped layer is modified by a protrusion as induced by the interaction of the aluminum with the phenol. The side views display that the protrusion is formed on the opposite side of the molecule position. The largest and smallest separation distances between the phenol and the graphene are 3.8 Å and 3.7 Å, respectively, while the distance from the molecule to the aluminum atom is 5.3 Å.

The relaxed Model B2 is represented in Fig. 3. The top view in a) shows the hexagon of the molecule on top of the graphene layer with the aluminum atom lying at the center of the molecule hexagon. The side view in b) displays that the largest and smallest separation distances between the phenol and the graphene are 3.6 Å and 3.5 Å, respectively, while the distance from the molecule to the aluminum atom is 5.1 Å.

Table 1 In this table we show the binding energies corresponding to the interaction of phenol with intrinsic graphene

Configuration	Binding energy (eV)
A1	-0.082543252
A2	-0.083732751
A3	-0.084125758
A4	-0.072758363
A5	-0.080737343
A6	-0.058267748

Fig. 2 In this figure we show the relaxed structure in the parallel configuration B1, in (a) top view, in (b) and (c) side views



The phenol molecule preserves its planar shape however; the graphene layer exhibits a protrusion similar to model B1.

We show model B3 in the relaxed configuration in Fig. 4. The top view in a) shows the hexagon of the molecule on top of the graphene layer with the aluminum atom being outside the center of the molecule hexagon. The oxygen atom occupies the left hand side of the molecule. The side view in b) displays that the separation distance between the phenol and graphene is 3.5 Å while the distance from the molecule to the aluminum atom is 5.1 Å. The phenol molecule is not distorted from its planar shape but the graphene layer exhibits a protrusion similar to models B1 and B2.

Model B4 of the parallel configurations is presented in Fig. 5. The top view in a) shows the oxygen atom at the farthest distance from the aluminum atom. One carbon atom of the phenol interacts with the aluminum with an attractive force inducing a protrusion in the graphene which in this case is near the phenol. The planar shape of the molecule is preserved. The lateral view in b) exhibits that the distance between the molecule and the aluminum is 2.3 Å, the largest and smallest distances between the molecule and the graphene are 4.2 Å and 3.9 Å, respectively. According to the separation distances, this model B4 favors the molecule chemical adsorption.

Configuration B5 is presented in Fig. 6. Initially the phenol is placed parallel to the layer with the oxygen on top of the aluminum. After the relaxation the layer exhibits a protrusion formed towards the molecule, the molecule is tilted 12 degrees with the position of the oxygen respect aluminum favoring the chemical bond. The bonding is a consequence of the interaction of the oxygen free orbitals with the non-occupied pz aluminum orbital. The O-Al bond length is 1.98 Å which indicates chemisorption. The total energy of the B5 configuration is lower compared with

those of B1-B4 models therefore we conclude that the parallel configurations have B5 as the most stable structure. In this geometry the hydrogen atom bonded to the oxygen is not coplanar to the phenol.

When results obtained for the interaction between phenol and graphene, in the parallel configurations, are compared with those corresponding to the interaction of phenol with the aluminum doped graphene we realize that B5 is the one with the smallest separation distance between the molecule and the layer, which indicates that the doping favors the chemisorption.

We turn to describe the interactions of graphene with phenol in the perpendicular configurations. As a first model we describe B6, the relaxed structure is displayed in Fig. 7. In this case the interaction of the graphene with the molecule is given through a hydrogen atom of the molecule and the aluminum. The top view in a) indicates that the molecule is on top of the aluminum atom. The protrusion due to the interaction between the graphene and the molecule is formed on the opposite side of the molecule position. The side view in b) exhibits the oxygen atom on top of the molecule, the separation distance between the hydrogen and the aluminum is 3.50 Å.

The next perpendicular model B7 is shown in Fig. 8. In the relaxed configuration the oxygen of the molecule is near the graphene layer. The side view in b) exhibits that the interaction of phenol with the layer is mainly through the oxygen and the aluminum, the separation distance is 1.97 Å which indicates chemical adsorption. We shall mention that the molecule planar shape is almost unaffected but the orientation is distorted from the perpendicular configuration (15.4°). Similar to the parallel models the graphene exhibits a protrusion directed toward the molecule as a result of the interaction between the layer and the molecule.

The relaxed structure of model B8 is shown in Fig. 9. The top view a) exhibits how the phenol molecule is displaced from

Fig. 3 In this figure we display model B2 in the relaxed state, in (a) top view, in (b) and (c) side views

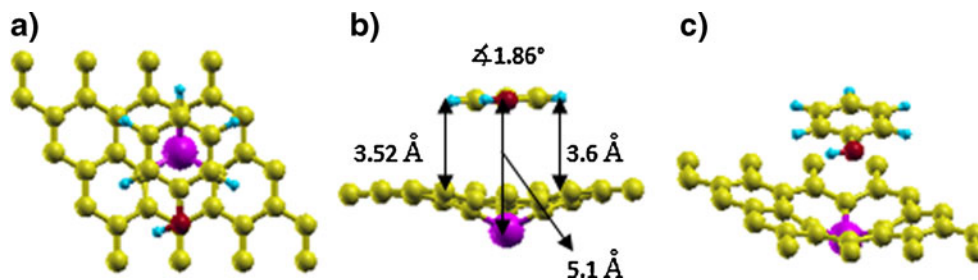
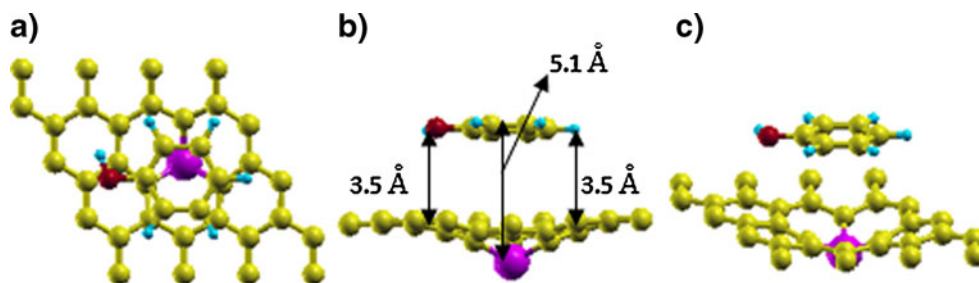


Fig. 4 This figure exhibits the relaxed B3 configuration, in (a) top view, in (b) and (c) side views



the initial perpendicular position. In the model, the side views b) and c) show that two hydrogen atoms are placed near the aluminum atom and after the relaxation the molecule deviates from the perpendicular geometry, with the molecule making an angle of 18.15° with a vertical line. The protrusion induced at the aluminum site because of the interaction with the phenol is in the same side of the molecule and is near the molecule.

When results obtained for the interaction between phenol and graphene in the perpendicular configurations are compared with those corresponding to the interaction of phenol with the aluminum doped graphene we realize that B7 is the one that displays the smallest separation distance between the molecule and the layer, which indicates that the doping favors the bonding.

In all configurations, after the geometric relaxation, no significant changes are obtained in the structural parameters of the phenol molecule (binding angles and distances). However, in configurations B5 and B7, where chemical bond is formed between oxygen atom of phenol and the aluminum of the surface, small changes are detected in the C-O binding distance as well as C-C-O and C-O-H binding angles, this is expected since these atoms are involved in the binding.

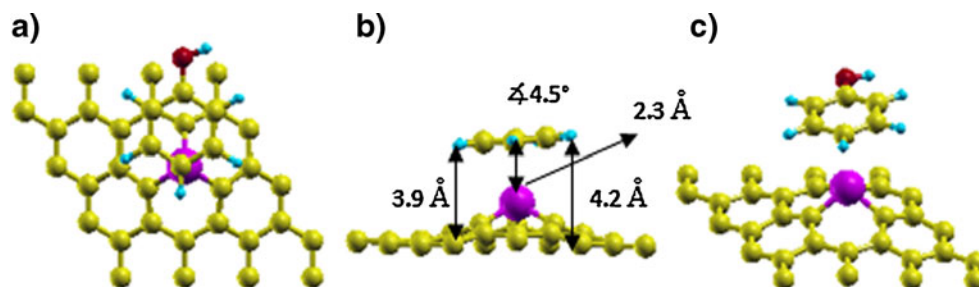
Binding energy

Our studies include calculations of the binding energies of the adsorbed molecule with stable structures. To determine these energies [21] we use

$$E_b = E_{\text{graphene-phenol}} - E_{\text{graphene}} - E_{\text{phenol}}, \quad (1a)$$

$$E_b = E_{\text{Al-graphene-phenol}} - E_{\text{Al-graphene}} - E_{\text{phenol}}. \quad (1b)$$

Fig. 5 This is the relaxed B4 structure, in (a) top view, in (b) and (c) side views



In Eq. 1a the first term corresponds to the total energy of the system composed of the graphene layer interacting with the phenol molecule, the second term represents the total energy of the graphene layer and the third term corresponds to the isolated phenol molecule. In Eq. 1b the first term corresponds to the total energy of the system composed of the aluminum doped graphene layer in the presence of the phenol molecule, the second term represents the total energy of the aluminum doped graphene layer and the third term corresponds to the isolated phenol molecule.

Table 1 shows binding energies corresponding to the interaction of phenol and the intrinsic graphene, with configurations A1, A2, and A3 displaying the largest energies. In these configurations the phenol molecule is parallel to the graphene surface. Similar results have been reported on the adsorption of phenol on boron nitride sheets [22].

In the system composed of phenol and Al-doped graphene, values of the binding energies indicate that the doping favors the chemisorption of the phenol on the graphene layer. These energies are larger (of the order of eV) than those of the system composed by phenol and intrinsic graphene (binding energies are of the order of meV, see Table 1). Results of the binding energies show that the largest binding energy corresponds to model B7, see Table 2.

Using the energies of the relaxed atomic configurations (B1 – B8) we have also calculated the relative energy difference. Using these results we plot the surface potential energy, which is reported in Fig. 10. The graph shows two minima which indicate one stable and one metastable structural configuration. It is apparent that configuration B7 yields the most stable structure, while B5 represents a metastable geometry. Results of the binding energies and relative total energies suggest B7 as the ground state of the system.

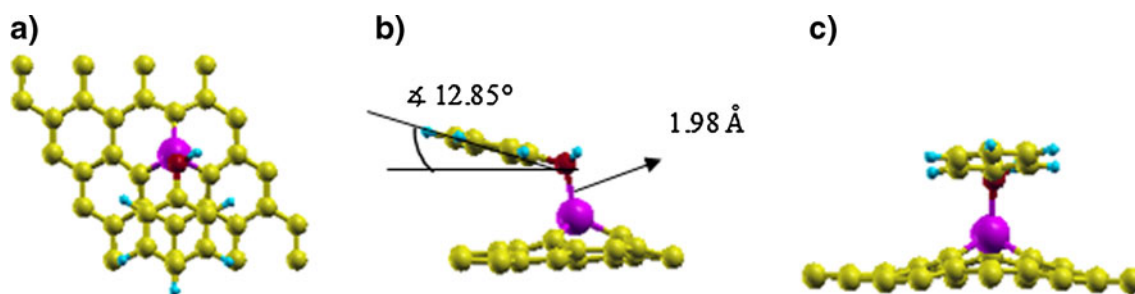


Fig. 6 In this figure structure B5 is presented, (a) shows the top view, (b) and (c) display two side views

Fig. 7 This figure presents the relaxed model B6, in (a) top view, in (b) and (c) side views

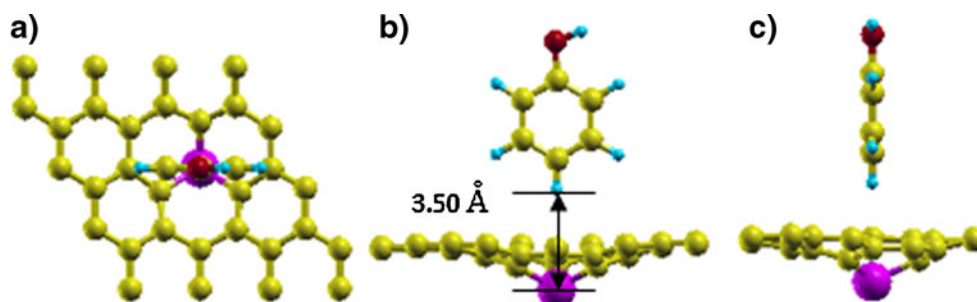


Fig. 8 The figure represents the relaxed configuration B7, in (a) top view, in (b) and (c) side views

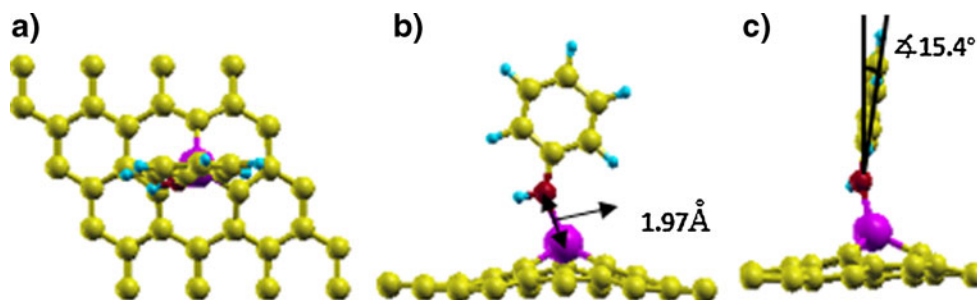


Fig. 9 The figure shows the relaxed configuration B8, in (a) top view, in (b) and (c) side views

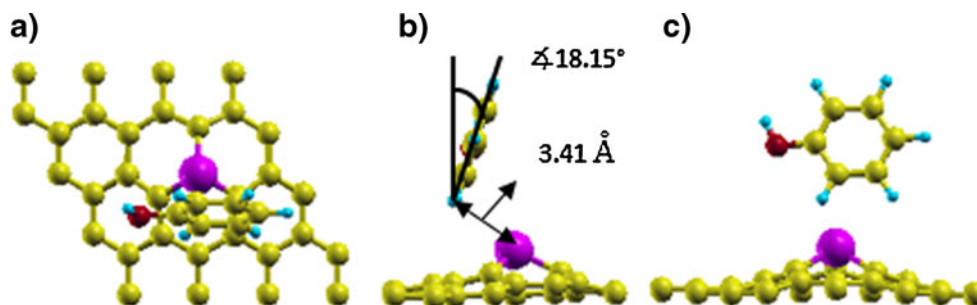


Table 2 In this table we show the binding energies for the most stable configurations

Configuration	Binding energy (eV)
B1	-1.80633421
B2	-1.804099098
B3	-1.798857314
B4	-2.365445433
B5	-2.515510910
B6	-1.801262118
B7	-2.594087158
B8	-1.950325056

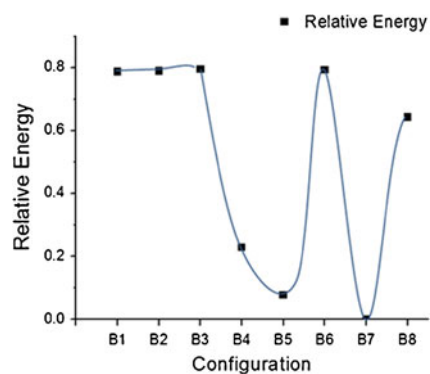
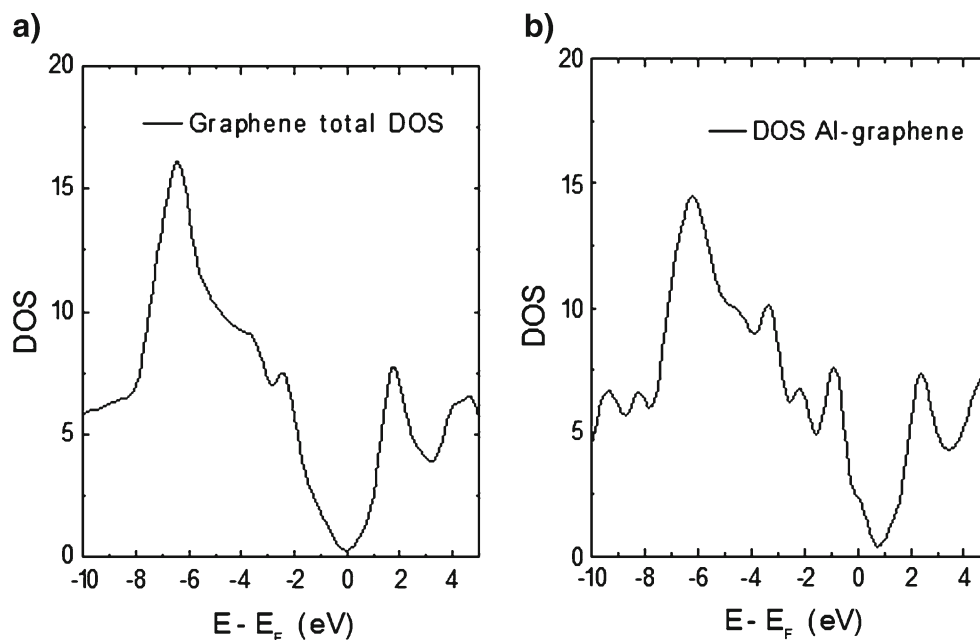


Fig. 10 The plot represents the relative energy with the reference being B7

Fig. 11 Figures show the DOS for the intrinsic graphene (a) and Al-doped-graphene (b) layers



Density of states

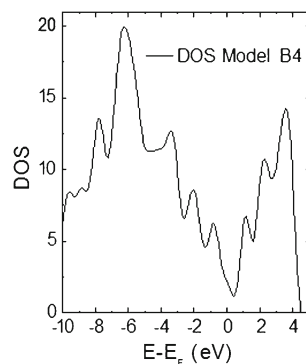
In this section we present calculations of the total density of states (DOS) and partial DOS for the interaction of phenol with graphene. We start by considering the clean intrinsic graphene and then the aluminum doped graphene without phenol molecule interaction. Afterward we discuss the interaction of phenol with the aluminum doped graphene.

Figure 11a shows the total DOS of the relaxed clean intrinsic graphene and Fig. 11b displays the DOS of the aluminum doped graphene layer using a (4x4) unit cell. For the clean intrinsic graphene, we obtain that the atomic configuration shows zero gap semiconductor characteristic. Similar behavior has been found for the intrinsic graphene layer previously reported by Chi, Zhao [15] and Leenaerts, Partoens, and Peeters [23], for a similar (4x4)-periodicity. Considering that the aluminum doped graphene (4x4) supercell has an unpaired electron density at the aluminum site,

we expect that the adsorption of a phenol molecule, with additional valence electrons, will be adsorbed on graphene.

Figure 12 shows the total DOS when the phenol molecule is adsorbed on graphene in the configuration B4. In this case, the surface is affected by a charge distribution which produces a state in an almost parallel configuration. In Fig. 13, we show the partial DOS of the relaxed B4 geometry. At the upper panel (a) we plot the DOS corresponding to the aluminum graphene system. Below this in (b) we display the corresponding partial DOS for the aluminum atom. In (c) we display the partial DOS of oxygen. The partial DOS corresponding C atoms of phenol are plotted in (d), and finally in (e), we plot the partial DOS of hydrogen atoms. To describe the contributions of the partial DOS to the total DOS we consider two regions of energies; one below and another above the Fermi energy (E_F). At energies below E_F the shape of the total DOS is originated from the Al 3p orbitals and phenol C 2p orbitals. Al 3s orbital contributes in a less important amount. On the other hand, C 2s and H 1s orbitals contributions are unimportant. At energies above E_F the most important contribution to the total DOS comes from the phenol C 2p orbitals. H 1s and Al 3p orbitals contribute in a less important amount. It is apparent that the zero gap energy characteristic is preserved.

Fig. 12 We show the total DOS for model B4



Finally, in Fig. 14, we show the total DOS of the relaxed structure of model B7 which is the ground state geometry. Considering again that the aluminum doped graphene (4x4) supercell has an unpaired electron density at the aluminum site, we expect that the adsorption of a phenol molecule on the graphene will take place, as additional valence electrons are present in the molecule. A comparison between the total DOS of the aluminum doped graphene and the total DOS of the structure with the presence of the molecule shows that

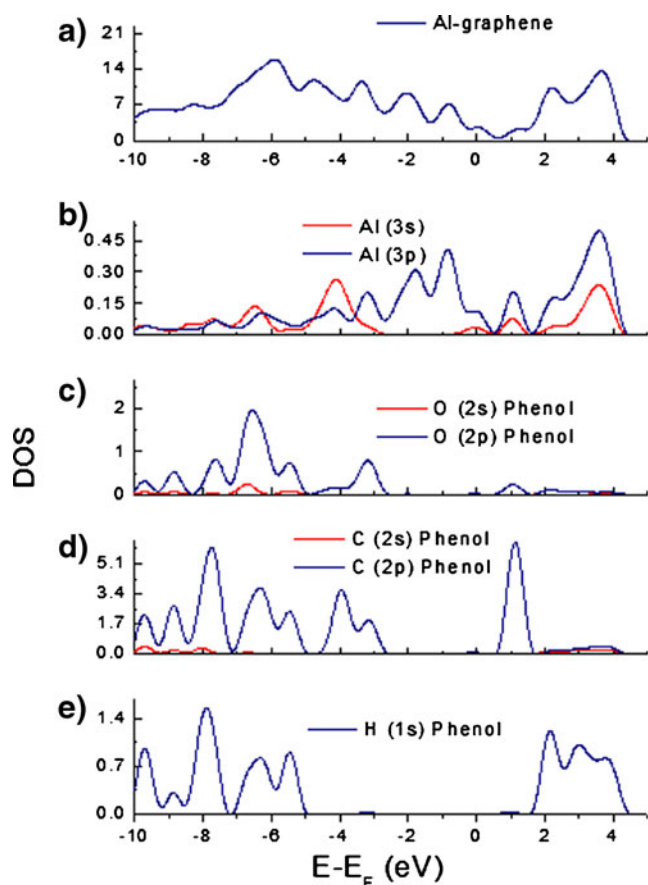


Fig. 13 This figure displays the partial DOS of B4 (a) Al-graphene graph, (b) Al (3s) and Al (3p) graph, (c) O (2s) Phenol and O (2p) Phenol graph (d) C (2s) Phenol and C (2p) Phenol graph, and (e) H (1s) Phenol graph

the interaction of the molecule with the graphene layer modifies the total DOS structure. This is a consequence of the adsorption of the molecule at the aluminum site. To complement our discussion we present in Fig. 15 the partial DOS for model B7. In the upper panel (a) we display the Al-graphene system in the absence of any molecule. Panel (b) represents the p and s aluminum orbitals. Panel (c) is

Fig. 14 This figure displays the DOS for model B7

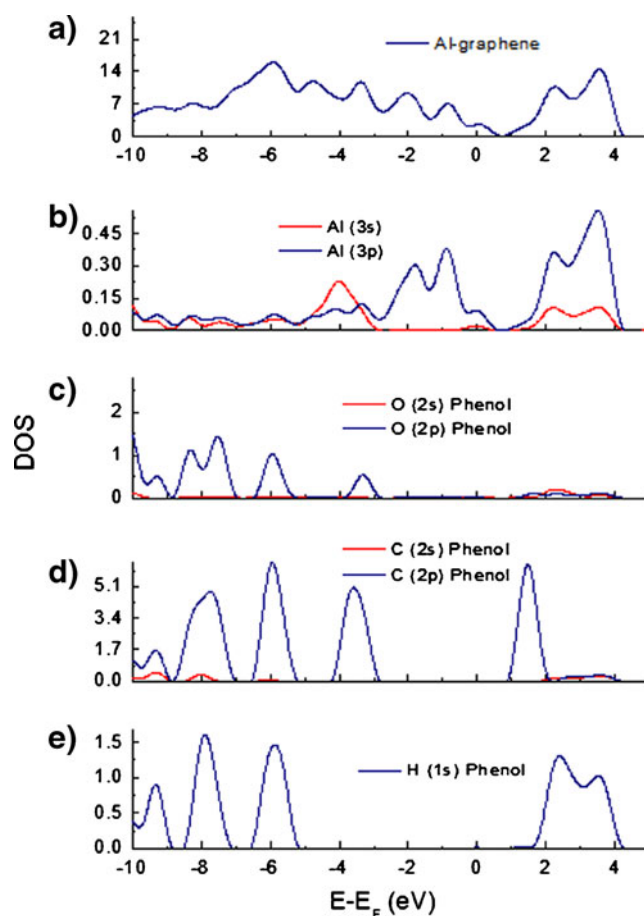
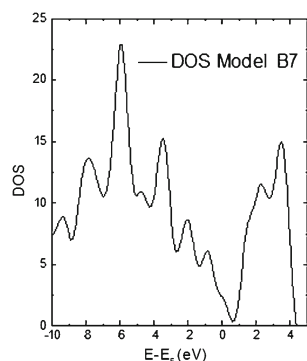


Fig. 15 The figure shows the partial DOS for model B7 (a) Al-graphene graph, (b) Al (3s) and Al (3p) graph, (c) O (2s) Phenol and O (2p) Phenol graph (d) C (2s) Phenol and C (2p) Phenol graph, and (e) H (1s) Phenol graph

devoted to the projected orbitals of the oxygen atom. In (d) we plot the partial DOS corresponding to the carbon atoms of the molecule, and finally in (e) we show the partial DOS of hydrogen. We describe the contributions of the partial DOS to the total DOS, in a similar fashion as done above, two regions of energies are invoked; one below and another above E_F . Similar to the results of model B4, at energies below E_F the shape of the total DOS is originated from the Al 3p orbitals and phenol C 2p orbitals. Al 3s contributes in a less important amount. On the other hand, C 2s and H 1s orbitals contributions are unimportant. At energies above E_F the most important contribution to the total DOS comes from the phenol C 2p orbitals. H 1s and Al 3p orbitals also contribute but O orbitals do not contribute. We shall mention that the absence of an energy gap is preserved after the phenol adsorption, however, the density of states at the Fermi level is somewhat modified as compared with the intrinsic system.

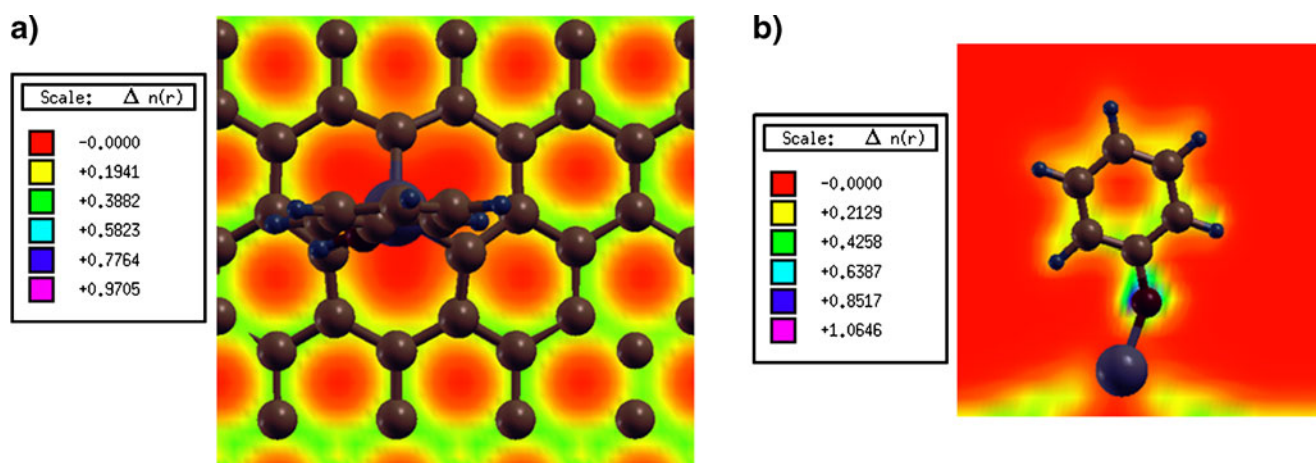


Fig. 16 We display the charge density of configuration B7. In the left panel (a) we present the top view while in right panel (b) a side view

Charge density distribution

To explore if in configuration B7 there is formation of a bond between the oxygen and the aluminum, we have calculated the charge density, as displayed in Fig. 16. In the left panel of the figure we show a top view of the phenol-graphene system and in the right panel a side view of the system. The structure of the charge distribution shows that a bond is formed between the oxygen of the phenol and the aluminum of the graphene. Considering the fact that these two atoms make a covalent-type of bonding, we conclude that the chemical adsorption of phenol is energetically and kinetically favorable. Figure 16b shows that the hydrogen atom, bonded to the oxygen, is not seen since this is not coplanar to the molecule. This is because the bonding between the oxygen and the aluminum atoms generates a change in the O-H angle in such a way that the hydrogen atom ends out of the phenol plane.

Conclusions

We have presented studies of the interaction between phenol and graphene in two cases: one for the intrinsic system and the other when the system is doped with aluminum. Studies have been done using first principles total energy calculations within the periodic density functional theory. A 4x4 periodicity has been used to explore the adsorption of a phenol molecule on graphene. We have considered different models and relax the atomic structures. The ground state model B7 displays the direct interaction between the oxygen and the aluminum with a bond length of 1.97 Å. We have used the relaxed coordinates to determine binding energies, density of states (DOS), partial DOS and charge distribution. The total DOS of the phenol—Al-doped graphene

system reveals that the electronic structure is affected with only small changes as compared with the intrinsic system, but the zero gap energy is preserved. In general results indicate that indeed model B7 is the ground state and the chemical adsorption of the phenol molecule is energetically and kinetically favorable.

Acknowledgments This work was partially supported by projects: Vicerrectoría de Investigación y Estudios de Posgrado - Benemérita Universidad Autónoma de Puebla (CHAE-ING12-G, EXC11-G), Cuerpo Académico Ingeniería en Materiales (BUAP-CA-177), Cuerpo Académico Física Computacional de la Materia Condensada (BUAP-CA-194) and. The work of G.H.C. was partially supported by Consejo Nacional de Ciencia y Tecnología (83982).

The authors would like to acknowledge the National Supercomputer Center (CNS) of Instituto Potosino de Investigación Científica y Tecnológica, Asociación Civil (IPICyT, A. C.) for supercomputer facilities. Calculations have been also performed at the Computer Center of the Instituto de Física “Ing. Luis Rivera Terrazas” – Benemérita Universidad Autónoma de Puebla.

References

1. Geim AK, Novoselov KS (2007) *Nature Materials* 6:183–191
2. Ihn T, Güttinger J, Molitor F, Schnez S, Schurtenberger E, Jacobsen A, Hellmüller S, Frey T, Dröscher S, Stampfer C, Ensslin K (2010) *Materials Today* 13:44–50
3. Leenaerts O, Partoens B, Peeters FM (2008) *Phys Rev B* 77 (125416):1–6
4. Sutter P (2009) *Nat Mat* 8:171–172
5. Young JA (2007) *J Chem Educ* 84:759
6. Fraser CA (1921) *J Phys Chem* 25:1–9
7. Tripathi DG (printed and published) (2008) In: Roy A (ed for and on behalf of Tulip Diagnostics(P) Ltd) *J Hyg Sci I(IV)*:1–16
8. Tilley FW, Schaffer JM (1926) *J Bacteriol* 12:303–309
9. McDonnell G (1999) *Denver Russell A. Clin Microbiol Rev* 12:147–179

10. Kim KS, Choi SJ, Ihm SK (1983) *Ind Eng Chem Fundam* 22:167–172
11. Hamaidi-Maouche N, Bourouina-Bacha S, Oughlis-Hammache FJ (2009) *J Chem Eng Data* 54:2874–2880
12. Zuo X, Peng C, Huang Q, Song S, Wang L, Li D, Fan C (2009) *Nano Res* 2:617–623
13. Seredych M, Bandosz TJ (2009) *Mat Chem and Phys* 113:946–952
14. Seredych M, Bandosz TJ (2011) *Chem Eng J* 166:1032–1038
15. Chi M, Zhao YP (2009) *Comp Mat Sci* 46:1085–1090
16. Chakarova-Käck SD, Borck Ø, Schröder E, Lundqvist BI (2006) *Phys Rev B* 74(155402):1–7
17. Ao ZM, Yang J, Li S, Jiang Q (2008) *Chem Phys Lett* 461:276–279
18. Baroni S, Dal Corso A, de Gironcoli S, Giannozzi P, Cavazzoni C, Ballabio G, Scandolo S, Chiarotti G, Focher P, Pasquarello A et al (<http://www.pwscf.org>)
19. Perdew JP, Burke K, Ernzerhof M (1996) *Phys Rev Lett* 77:3865–3868
20. Sholl DS, Steckel JA (2009) *Density Functional Theory, A Practical Introduction*, 1st edn. Wiley, New York, p 56
21. Mao Y, Yuan J, Zhong J (2008) *J Phys Condens Mater* 20(115209):1–6
22. Galicia-Hernández JM, Hernández-Cocoletzi G, Chigo-Anota E (2011) *J Mol Model*. doi:10.1007/s00894-011-1046-z
23. Leenaerts O, Partoens B, Peeters FM (2009) *Phys Rev B* 79(235440):1–5